Biological Procedures Online

METHODOLOGY

Open Access

Improved ChIP Sequencing for H3K27ac Profiling and Super-Enhancer Analysis Assisted by Fluorescence-Activated Sorting of Formalin-Fixed Paraffin-Embedded Tissues

Nenggang Jiang[1], Zhihao Wen[1], Huan Tao[2] and Hongyan Liao[1*]

Abstract

Archived clinical formalin-fixed paraffin-embedded tissue (FFPE) is valuable for the study of tumor epigenetics. Although protocol of chromatin immunoprecipitation coupled with next generation sequencing (NGS) (ChIP-seq) using FFPE samples has been established, removal of interference signals from non-target cell components in the samples is still needed. In this study, the protocol of ChIP-seq with purified cells from FFPE lymphoid tissue of nodal T follicular helper cell lymphoma, angioimmunoblastic type (nTFHL-AI) after fluorescence-activated cell sorting (FACS) was established and optimized. Essential steps included single cell preparation, heat treatment enhancing antigen retrieval and labeling, cell sorting, chromatin shearing, ChIP and NGS. Through assistance of FACS, we successfully isolated tumor cells from FFPE lymph node samples of nTFHL-AI and profiled super-enhancers (SEs) mapping by enrichment of H3K27ac signals. The data indicated that the SEs mapping of the sorted cells was different from that of the entire unsorted tissue sample. The H3K27ac signals with cell lineage specificity from background cell components were successfully removed, and the remaining SEs mapping was more similar to T follicular helper cell in an unsupervised clustering analysis, rather than the primary tissue. In addition, we also evaluated the protocol using cultured pure cell lines, and the results indicated that the sequencing data obtained through this protocol had high fidelity and reproducibility. These results show that ChIP-seq for H3K27ac profiling and SEs mapping assisted by FACS with pathological FFPE tissue is available for research of histone modification. Precise epigenetic characteristics of the tumor cell can be described with this protocol.

Keywords Chromatin immunoprecipitation coupled with sequencing, Fluorescence-activated cell sorting, Formalin-fixed paraffin-embedded tissue, H3K27ac, Super-enhancers, Tumor

*Correspondence:
Hongyan Liao
hongyanliao@wchscu.cn
[1]Department of Laboratory Medicine, West China Hospital of Sichuan University, Chengdu 610041, China
[2]Department of Hematology, West China Hospital of Sichuan University, Chengdu 610041, China

Introduction

Transcriptional regulatory elements in complex genomes are key players that drive the aberrant transcription of oncogenes in cancer [1]. Among them, enhancers are classical activating regulatory elements that recruit transcription factors (TFs) and chromatin-associated regulatory complexes [2]. Superenhancers (SEs) are large clusters of transcriptional enhancers, consist of a long genomic domain composed of an enhancer cluster occupied by high levels of H3K4me1, H3K27ac, p300 or master TFs, and act synergistically to strongly activate oncogene transcription [1, 3, 4]. Identification of SEs and understanding the functional mechanisms by which SEs regulate target gene expression could help to reveal cancer development and direct strategies applications in cancer therapy [5].

Chromatin immunoprecipitation (ChIP) coupled with next generation sequencing (NGS) (ChIP-seq) has long been the primary and gold standard method for studying the modification and regulation on DNA of the regulatory elements [6]. By precipitating the antigen-antibody complex, the DNA fragments that incorporate with special protein, such as histone and transcription factors, can be captured, and then the captured DNA can be sequenced by high throughput technologies and annotated as particular genes [7, 8]. The method of ChIP by H3K27ac with fresh cell line or tissue has been well established, but in most real clinical settings, only the archived formalin-fixed paraffin-embedded tissue (FFPE) are available, which is challenging regarding to antigen-antibody reactions and extraction of high quality DNA because of the heavy cross-link [9, 10]. Furthermore, many pathological tissues from the tumor sites are complexed with not only tumor cells but also numerous other types of normal or reactive cells, known as the tumor microenvironment [11]. Considering the key regulatory regions including SEs are highly committed to the cell lineage [12], the maps of histone modifications gained from the entire FFPE tissue may be substantially complicated with the contributions from both the neoplastic and nonneoplastic cells. Thus, the epigenomic landscape of the targeted tumor cells could be misinterpreted due to the interference from the nonneoplastic cellular components. A few studies have described the ChIP protocol with FFPE tissue in detail [13–16], but none of them covered on how to get the histone modification profile of a single purified cell population within the FFPE tissue. Although macro- or microdissection can be used to select and cut the aimed region with enriched cellular components in tumor tissues, fluorescence-activated cell sorting (FACS) by flow cytometry (FCM) remains the most efficient and inexpensive method for cell purification. The method of ChIP-seq after FACS with fresh tissue has been used in some investigations [17, 18], whereas sorting single cell populations from FFPE tissue for ChIP-Seq has not yet been described due to FFPE sample not being ideal material for flow analysis.

In this study, we established a protocol for ChIP-seq with purified cells from the lymphoid FFPE tissue of patients with nodal T follicular helper cell lymphoma, angioimmunoblastic type (nTFHL-AI) after FACS. The signals of SEs were mapped by H3K27ac enrichment, and the effect of cell isolation on mapping was assessed. While tested on a single tumor type, this procedure is potentially applicable to a wide variety of tumors with the replacement of tumor-specific markers for FACS. We believe that the current reported method could help promote the application of ChIP-seq to epigenetic studies of archived FFPE tumor tissues, which will further enlighten the mechanism investigation and therapy development of cancer.

Materials and Methods

Methods Overview

A schematic overview of the ChIP-Seq protocol is shown in Fig. 1.

FFPE Tissues

Four deidentified FFPE tissue blocks were utilized in this study, including one lymphoid tissue sample from a tonsil with reactive hyperplasia and three from patients with nTFHL-AI (named AITL1, AITL2, and AITL3; Supplementary Table 1). All patients were clinically diagnosed, and the archived tissues were reviewed by pathologists to confirm the histologic diagnosis. Approval was obtained from the Ethics Committee of West China Hospital. The procedures used in this study adhered to the tenets of the Declaration of Helsinki.

Preparation of FFPE Cell Blocks

Fresh lymphoid tissue was incubated in 10% buffered formalin solution overnight at room temperature for fixation. Next, the fixed tissue was routinely dehydrated in a graded ethanol series (70%, 80%, 90%, and 100%) and embedded in paraffin through an automated tissue processor (Tissue-Tek VIP, Sakura).

To prepare an FFPE block from fresh cell line, twenty million OCI-LY7 cells (DSMZ, ACC 688), which were maintained in a T25 flask with RPMI (Life Technologies, Cat#: 11875-119) along with 1% penicillin–streptomycin and 10% fetal bovine serum (FBS) (Thermo Fisher, USA) at 37 °C and 5% CO_2, were washed with PBS. After incubation for 10 min in 1 ml of 10% buffered formalin, the cells were pelleted in a 0.5 ml microcentrifuge tube (Bio-Pioneer, GEXC-0.6NL) by centrifugation at 10 000 ×g for 5 min. Then, the cell pellet was fixed again and embedded in paraffin following the protocol for processing clinical tissues.

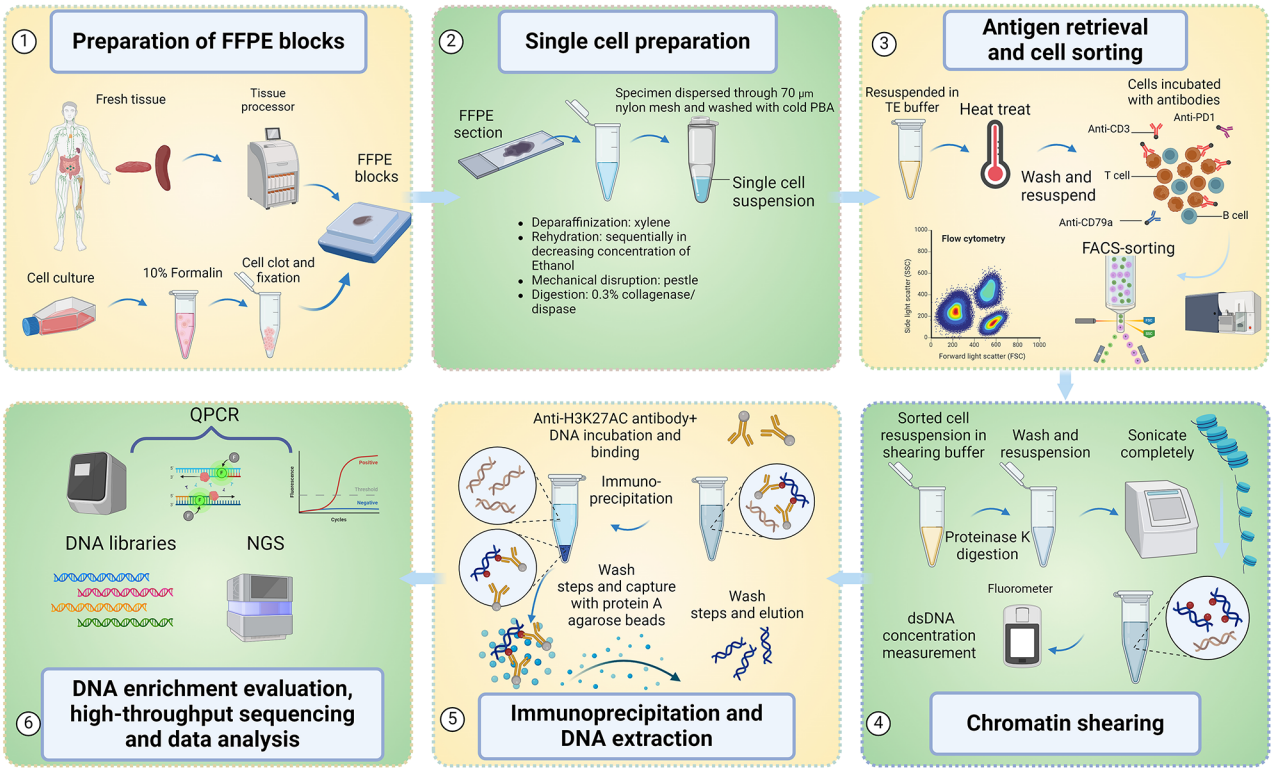

Fig. 1 Schematic overview of the improved FACS-assisted ChIP-seq protocol for H3K27ac profiling of FFPE samples

Single-Cell Preparation from FFPE Tissues and Cell Sorting by FACS

Thick sections of 50 µm thickness were prepared from FFPE tissues. Single cells were prepared from several sections through deparaffinization, rehydration, mechanical disruption, 0.3% collagenase/dispase digestion and filtering according to our previously established methods [19].

The prepared single cells were resuspended in 250 µl of TE buffer (1.0 mM EDTA, 10 mM Tris-HCl, pH 8.0) and heated at 50 °C for 60 min. Then, the cell suspension was transferred into a 5 ml Falcon tube (Life Sciences, Cat#: 352054), and the cells were washed with 4 ml of PBA and pelleted again by centrifugation. After being resuspended in 400 µl of PBA, the cells were incubated with 10 µl of FITC-labeled PD1 (BioLegend, Cat#: 329903), 10 µl of PE-labeled CD79a (BD Pharmingen, Cat#: 555934) and 10 µl of purified polyclonal rabbit anti-human CD3 (Dako, Cat#: IS503) overnight in a 4 °C refrigerator. After incubation, the cells were washed twice by adding 4 ml of PBA and centrifuged at 500 ×g for 5 min. Then, the cells were incubated with 5 µl of Alexa Fluor 647-labeled anti-rabbit IgG antibody (Molecular Probes, Cat#: 4414 S) for 2 h in a 4 °C refrigerator, followed by washing once as above and resuspending in 500 µl of PBA. CD3 + PD1 + cells were sorted with a BD Aria III cytometer with Diva software.

Chromatin Shearing

The sorted cells were pelleted by centrifugation at 500 × g for 5 min and resuspended in 250 µl of shearing buffer (0.3% SDS, 10 mM EDTA and 50 mM Tris-HCl). Proteinase K was added into the cell suspension to a final concentration of 40 ng/µl. After incubation for 2–3 min at room temperature (20–25 °C), the serine protease inhibitor AEBSF (Santa Cruz Biotechnology, Cat#: sc-202041) was added to a final concentration of 2 µg/µl to inactivate protease K. The cells were washed twice with precooled PBS and pelleted by centrifugation at 6 000 × g for 3 min each time, after which the cells were resuspended in 500 µl of shearing buffer, and 10 µl of 50× protease inhibitor (cOmplete Protease Inhibitor Cocktail, Roche, Cat#: 11697498001) was added. Sonication was carried out in 1.5 ml Eppendorf tubes using a Sonicator 4000 (Qsonica Misonix) (Supplementary Methods: Chromatin shearing). The concentration of dsDNA in the sonicated chromatin sample of the supernatant was measured via a Qubit 3.0 fluorometer (Fisher Scientific) with a Qubit dsDNA HS Assay Kit (Fisher Scientific, Cat#: Q32854), and the fragment size was checked via electrophoresis on a 1.5% gel.

Immunoprecipitation and DNA Extraction

Chromatin with at least 300 ng dsDNA was used for each immunoprecipitation and diluted 3-fold with dilution

buffer (1.5% Triton X-100, 5 mM Tris-HCl pH 8.0 and 225 mM NaCl) containing 1× proteinase inhibitor. For preclearing, forty microliters of protein A agarose beads (Roche) were washed 3 times, each time centrifuged at 1000 × g for 1 min in 1 ml of low-salt buffer (0.1% SDS, 1.0% Triton X-100, 2.0 mM EDTA, 20 mM Tris-HCl, pH 8.1, and 150 mM NaCl), and the supernatant was discarded. After the sonicated chromatin sample was incubated with the washed beads for 1 h at 4 °C, approximately 1/10 the volume of the precleared chromatin was kept, from which the DNA was extracted as input, and the remaining chromatin was incubated with 8 μg of anti-H3K27ac antibody (Abcam, Cat#: ab4729) overnight at 4 °C on a rotating platform. After that, the chromatin-antibody compound was captured by 50 μl of washed protein A agarose beads through incubation for 3 h at 4 °C. The beads were subsequently washed, and the captured DNA was extracted via kits according to the manufacturer's instructions (Supplementary Methods: Beads washing and DNA extraction after immunoprecipitation).

DNA Enrichment Evaluation

Quantitative PCR (qPCR) was performed with KAPA SYBR® FAST Universal 2× qPCR Master Mix (Kapa Biosystems, Cat#: KK4602) on a C1000 Touch thermal cycler (Bio-Rad) to check the DNA fragments captured by H3K27ac. The primers used are listed in Supplementary Table 2.

DNA Immunoprecipitation with Freshly Cultured Cells

For the freshly cultured cell line, DNA was immunoprecipitated with an anti-H3K27ac antibody via a ChIP assay kit (Millipore, Cat#: 17–295) according to the manufacturer's protocol.

High-Throughput Sequencing

DNA libraries were prepared via KAPA Hyper Prep Kits (Roche, Cat#: 07962347001) according to the manufacturer's protocols. Single-read sequencing of 51 bp was performed on the Illumina HiSeq2500 instrument, and approximately 50 M reads per sample were obtained.

Data Analyses

The quality of the sequencing data was evaluated via FSATQC. The raw sequencing reads were aligned with the *Burrows–Wheeler Aligner* against the reference genome Hg19 with default settings to obtain visualization files and a list of peaks. The genome was divided into bins of 100 kb for H3K27ac marks, and the number of mapped reads in the individual bins was calculated. The read count per bin was normalized to 25 million mapped reads. Pearson correlation analysis of the read counts between paired sequencing data was performed.

To define SEs, regions of ChIP-seq enrichment over background were identified with peak-finding algorithm of the MACS3 [20]. MACS peaks of H3K27ac were used as constituent enhancers for SEs identification. Enhancers were stitched and SEs were identified using rank-ordering of superenhancers (ROSE) algorithm [3, 5].

Results

Evaluation of Cell Purification for nTFHL-AI Lymphoid Tissues by FACS

In nTFHL-AI lymphoid tissues, tumor T cells are often in the minority and frequently obscured by other reactive lymphocytes. The percentage of neoplastic follicular T helper (Tfh) cells of the three nTFHL-AI cases was 18-35% at diagnosis (Supplementary Table 1). For T- and B-cell identification, the targeted antigens included the T-cell lineage-specific marker (CD3), B-cell lineage-specific intracellular molecules (CD79a), and PD1, which helps to enrich Tfh cells [21]. Labeling efficiencies of antigens for FACS after antigen retrieval with various temperature−time combinations, including 40 °C, 50 °C and 65 °C were tested. As a result, through antigen retrieval at 50 °C in TE buffer for 60 min and antibody labeling overnight, the lymphocytes could successfully be separated into the CD3 + T cell, CD79a + B-cell and CD3 + PD1 + population by FCM (Fig. 2). However, the antigen markers could not be labeled after treatment at 40 °C(data not shown), and 65 °C treatment in retrieval buffer resulted in heavily dissociation between histone and DNA in subsequent experiments, which is consistent with the results indicated in our previous study [19] and another reported protocol [13].

The Efficiency of Chromatin Shearing

To evaluate the effect of the procedure before sonication on chromatin fragment preparation, the quantity and size of DNA yielded from separated cells subjected to five different pretreatment procedures were measured, including the following conditions: I, without treatment; II, 50 °C treatment only; III, 50 °C treatment and proteinase K digestion; IV, proteinase K digestion only; and V, 65 °C treatment only (Fig. 3A). With 3 million cells isolated from FFPE lymphoid tissue, an average of 1.9 μg of dsDNA could be obtained under condition III (the total DNA input was 9.8 μg), which was significantly greater than that under all the other four conditions (all $p < 0.001$). Moreover, if the cells were pretreated with the other four procedures, the dsDNA yields were all less than 1.0 μg, which was only 1/2 to 1/3 of that with condition III. The dsDNA yield was the lowest if the cell sample was processed without any pretreatment (condition I). The chromatin fragment sizes of all processed samples were relatively consistent, as the sizes of most fragments ranged from 200 to 500 bp (Fig. 3B).

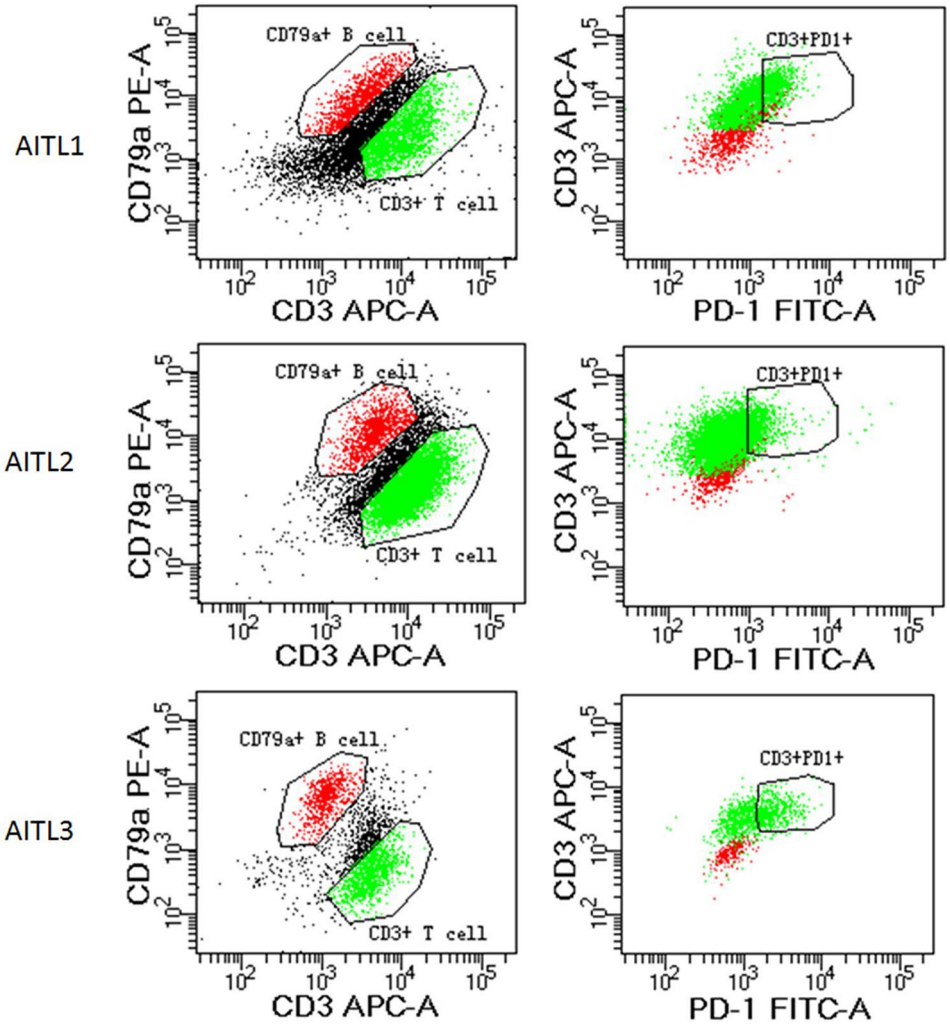

Fig. 2 Identification of cell populations from three FFPE tissues of nTFHL-AI by immunophenotyping after antigen retrieval

DNA Recovery and Target DNA Enrichment Efficiency of ChIP

The DNA recovery ratio, represented by the percentage of DNA captured by the anti-H3K27ac antibody within the input DNA, was calculated by the cycle threshold (Ct) value of qPCR. Additionally, the enrichment efficiency of the target genes (H3K27ac-positive genes [GAPDH and DRE13]) was compared to that of MYOD, the H3K27ac-negative gene (Fig. 3C). As a result, the percentages of all captured genes with all five protocols that used to treat the FFPE samples for ChIP were less than 4%. Treatment only with 50 °C incubation for antigen retrieval before chromatin shearing (condition II) yielded the highest percentage; however, the recovery ratios of GAPDH and DRE13 were only approximately 3.8- and 4.3-fold greater than that of MYOD, respectively (mean: 3.27% and 3.73%, respectively, versus 0.87%), indicating a low efficiency of target DNA enrichment. If 65 °C heat treatment was used for antigen retrieval, both the DNA recovery and enrichment of ChIP products were unacceptable. In a previous study [22], DNA enrichment by H3K27ac ChIP after incubation at 65 °C was successful; however, their protocol did not include FACS, and the incubation solution used was different from that used in our study. Notably, although sample digestion with proteinase K before shearing (condition III) reduced the DNA recovery ratio, the enrichment of target DNA was significantly improved, as the recovery ratios of GAPDH and DRE13 reached approximately 9.9- and 7.3-fold greater than that of MYOD, respectively (mean: 1.09% and 0.80%, respectively, versus 0.11%). Therefore, combining the results of the recovery ratio and target gene enrichment, the 50 °C heat treatment of antigen retrieval for FACS followed by proteinase K digestion before chromatin shearing outcompeted the other four conditions. With this protocol, H3K27me3-modified DNA could also be effectively enriched (Supplementary Fig. 1).

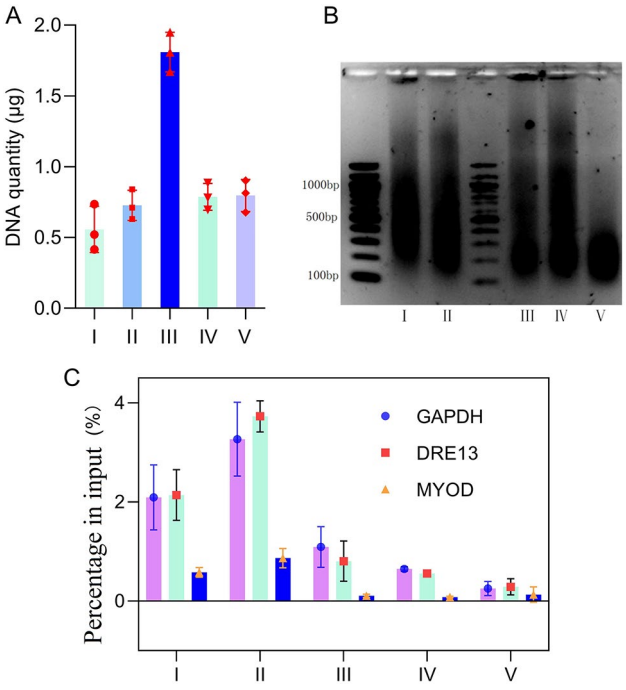

Fig. 3 Optimization of the FACS-assisted ChIP-seq sample preparation protocol using 3 million cells from FFPE tissue (tonsil). **A**, Bar graph showing the comparisons of dsDNA quantity yielded after sonication (data representing triplicate results); **B**, Representative gel electrophoresis showing the smear of fragmented DNA, indicating the DNA fragment size of chromatin after shearing. **C**, qPCR assay evaluating the relative recovery and enrichment of captured DNA by anti-H3K27ac antibody from FFPE lymphoid tissue with different protocols of sample treatment. Percentage in input (%) = 100*2^[input Ct–Log_2(start volume of ChIP chromatin sample/start volume of input chromatin sample)-ChIP Ct], given that all yielded DNA was used as a template for a pair of primers. I, without treatment; II, 50 °C treatment only; III, 50 °C treatment and proteinase K digestion; IV, proteinase K digestion only; V, 65 °C treatment only

Reproducibility of FACS-Assisted ChIP-Seq

To evaluate the performance of the current FACS-assisted ChIP-seq protocol, we compared the H3K27ac signals from the ChIP-seq data that generated from fresh cells and FFPE blocks prepared from cultured cell lines. As uneven distributions of cells in real tissues may introduce potential biases, the lymphoid samples were not used for this comparison. Notably, the resultant H3K27ac signal in the FFPE samples was highly correlated with that in the matched fresh OCI-LY7 cells ($r = 0.93$; Fig. 4A). Furthermore, repeats of the FFPE experiment based on OCI-LY7 were highly correlated ($r = 0.90$; Fig. 4B), indicating reliably high reproducibility. In contrast, the correlation between datasets generated from FFPE block of OCI-LY7 cells and fresh OCI-LY3 cells (DSMZ, ACC 761) was poor ($r = 0.54$; Fig. 4C), recapitulating the signal specificity. Overall, the current FACS-assisted ChIP-seq protocol demonstrated outstanding performance in H3K27ac profiling.

Identification of Tumor Type-Specific Enhancers and SEs in Sorted Cells

To evaluate the specificity and enrichment efficiency of the current protocol in aspects of SE signal identification and annotation, we checked the H3K27ac modification of genes that are specifically expressed by T and B cells. H3K27ac signals of B-cell-related genes (PAX5, BCL11A and BANK1) were enriched in unsorted lymphoid tissue. However, they were negative or slightly enriched in isolated CD3 + PD1 + samples, indicating that FACS contributes to depleting unwanted interfering cells (Fig. 5A). In contrast, H3K27ac signals of ICOS, CD28 and CTLA4, which are predominantly expressed by T cells as costimulating or inhibiting receptors [23, 24], were increased in enriched CD3 + PD1 + cells, confirming the important role of high expression of these genes in nTFHL-AI [25, 26]. Moreover, the signal intensity of MYC, which is not nTFHL-AI specific, was also lower in CD3 + PD1 + cells than in unsorted tissue, indicating its enrichment in background cells. Therefore, adopting the current FACS-assisted ChIP-seq method to profile the H3K27ac signals of FFPE tissues is desirable to reduce interference.

Signals with extraordinarily high and broad H3K27ac ChIP-seq peaks compared to average enhancers were identified as SEs by the ROSE algorithm [5, 27]. There were 975, 593 and 832 commonly identified SE signals

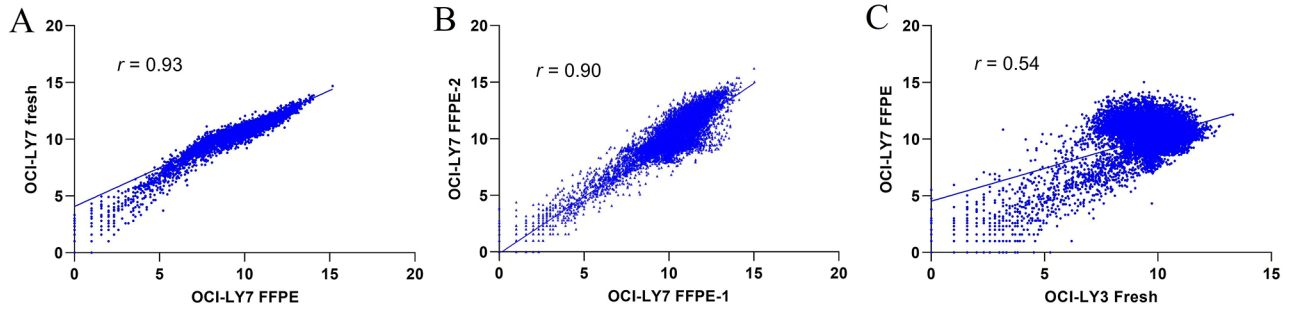

Fig. 4 Correlation analysis of the read numbers counted within each 100-kbp window from the ChIP-seq experiments. Linear regression was performed for each of the analyzed comparisons, and the Pearson correlation coefficient (*r*) of determination is indicated. **A**, Duplicated experiments of the same FFPE cell blocks; **B**, FFPE cell block and the corresponding fresh cell line; **C**, FFPE cell block and the different fresh cell line (OCI-LY3)

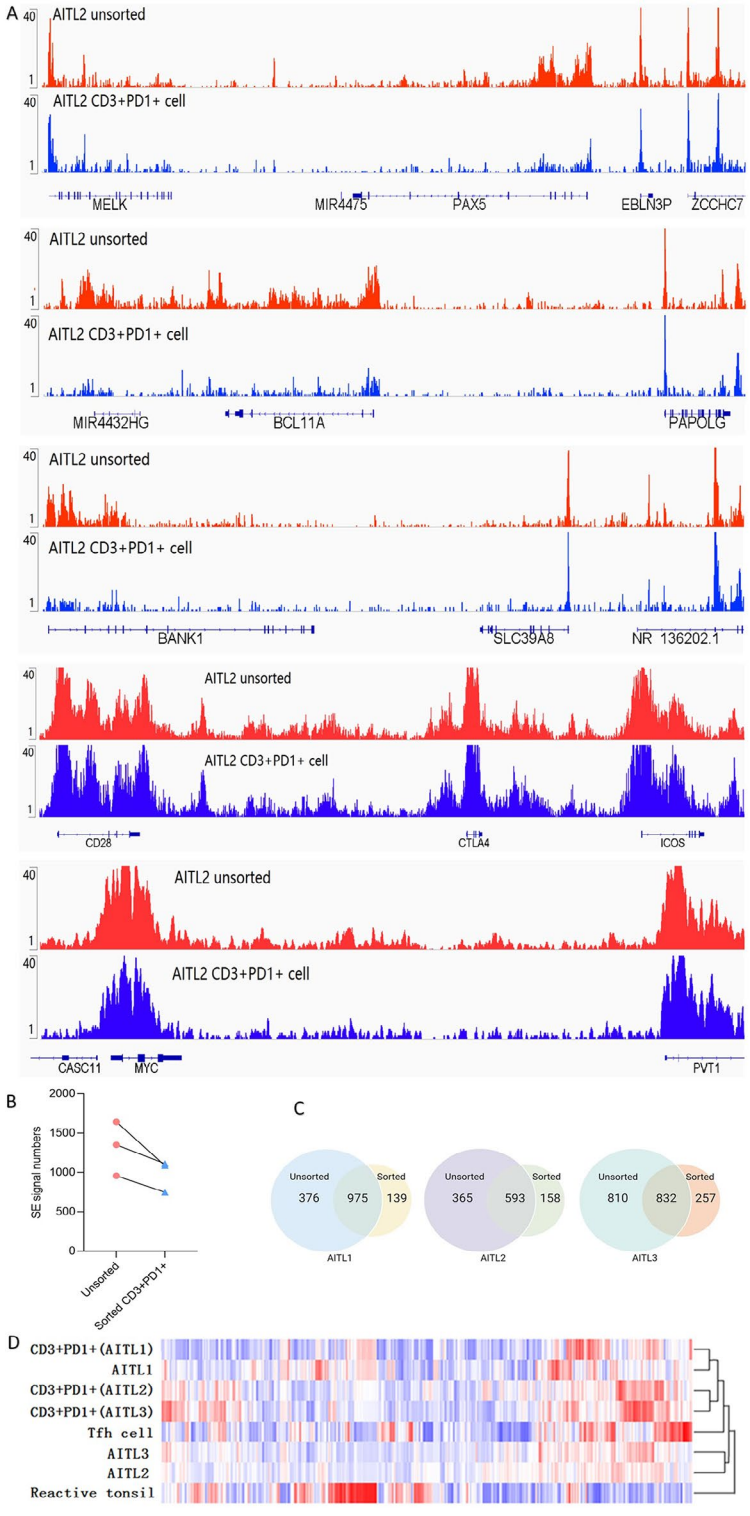

Fig. 5 Comparison of ChIP-seq datasets between lymphoid tissue and sorted cells. **A**, Representative IGV tracks of H3K27ac signals. Three B-cell-related genes (PAX5, BCL11A, and BANK1) were enriched in unsorted lymphoid tissue (AITL2) but were negatively enriched or slightly enriched in isolated CD3 + PD1 + cells. The enrichment of ICOS increased, whereas the enrichment of MYC decreased slightly after sorting. **B**, Comparison of SE numbers between unsorted tissue and the corresponding sorted samples of CD3 + PD1 + cells from the 3 nTFHL-AI lymphoid tissues. **C**, Venn diagram showing the common and separate SE numbers between unsorted tissue and the corresponding sorted CD3 + PD1 + cells from AITL1, AITL2 and AITL3. D, Hierarchical clustering of ChIP-seq datasets according to the identified SEs of 3 nTFHL-AI lymphoid tissues and the corresponding sorted CD3 + PD1 + lymphocytes

between two pairwise samples, and 139, 158 and 257 unique SE signals from the CD3 + PD1 + cell samples, respectively. The SE signal numbers from all three sorted specimens were consistently less than their matched unsorted correspondents (1114 vs. 1351, 751 vs. 958, 1089 vs. 1642, respectively; Fig. 5B and C).

Furthermore, unsupervised hierarchical clustering of the sample–sample correlations of the SE signals annotated for 8 samples was performed, including 3 sorted samples with CD3 + PD1 + lymphocytes from nTFHL-AI FFPE lymph nodes and their matched unsorted tissues, as well as a reactive tonsil tissue and a specimen of enriched fresh Tfh cells (CD4 + CXCR5+) (Fig. 5D). Notably, two of the unsorted nTFHL-AI tissues (AITL2 and AITL3) were grouped together with the reactive tonsil tissue, whereas their corresponding sorted CD3 + PD1 + lymphocyte samples were grouped together with Tfh cells. Taken together, these results indicated that the histone modification status of target tumor cells could be better described by the present FACS-assisted ChIP-seq method.

Discussion

In this study, we presented a procedure to enrich target cells from FFPE samples by FACS before ChIP and demonstrated its outstanding performance in target gene recovery, specificity, reproducibility and ability to identify H3K27ac and SE profiles. The decrosslinking procedure has been optimized to adapt for both FCM and immunoprecipitation. Through trials and tests, we showed that heat treatment with an adequate condition of temperature (50 °C) and time (1 h) not only enabled antigen labeling of the target cells but also increased histone–antibody binding. Another benefit of heat treatment is that it can increase yield when chromosome fragments are prepared, as has been demonstrated previously [28]. The sample was also digested by protease K to increase the enrichment efficiency of H3K27ac when the chromosome fragments were prepared. This step may help to expose the antigenic epitopes of histones [29]. However, the target DNA recovery rate after digestion with proteinase K was low, which may be due to proteinase K causing excessive decrosslinking of DNA and histones during antigen retrieval. Therefore, it may be necessary to attempt milder digestion by reducing the digestion time or concentration of proteinase K, which may decrease the impact on DNA capturing while ensuring histone antigenicity. By comparing the H3K27ac profiling between fresh sample and FFPE sample that containing identical cellular components, it was proved that the FACS-assisted ChIP-seq protocol did not alter histone signal mapping.

In our results, the mapping of H3K27ac was different between the sorted cells and the unsorted FFPE tissues from nTFHL-AI patients. nTFHL-AI originates from Tfh cells, but the enlarged lymph node is characterized by inflammatory background containing variable numbers of reactive T cell, B cell, histiocytes and plasma cells [30], rendering a small percentage of tumor cells scattered [31]. Thus, the SEs profiles of the tumor cells after sorting could be significantly different from the primary tissue and meanwhile more similar to Tfh cells, thus better reflecting histone modification and epigenetic characteristics of the tumor itself. This was confirmed by the elimination of B-cell specific signals and the retention of T-cell related signals. Moreover, SEs numbers of sorted cells were smaller than those of the unsorted tissues, which coincides with the fact of SEs as a cell-type specific chromatin regulatory marker [32]. In fact, this also holds true in multiple types of tumors, for example, melanoma and pancreatic cancer, where the TME may change dynamically and even show prognostic value [31, 33]. Another potential application of flow sorting before ChIP is to identify tumor cell subpopulations with heterogeneity in antigen expression through immunophenotyping, providing more detailed tumor epigenetic features. But achieving this purpose requires more antigen markers to be labeled simultaneously.

While these results are promising, certain limitations warrant further investigations. For specific research purposes, it is necessary to design a disease- and cell type-specific panel containing more markers for precise targeted cell sorting, but the varieties of structures and distributions of antigen markers in target cells may lead to differences in antigen retrieval efficiency. Only a few biomarkers were tested in this study, leading to the limitation that only CD3 and PD1 were used to identify Tfh cells in this study, while CD4 could not be retrieved and labeled (data not shown). Thus, the tumor cells may have been enriched but not purified. Additionally, when analyzing other types of tumor tissues, there may be different requirements for single-cell preparation, de crosslinking, and chromatin fragment preparation due to differences in tissue or chromatin structure. It might be needed to adjust experimental conditions such as temperature and duration based on this protocol.

In summary, the current study demonstrated the feasibility of performing ChIP-seq on target cells from FFPE samples with the assistance of FACS and the potential of an expanded application to multiple tumor types in a real-world clinical context for the purpose of research and therapy development. Additionally, more antigen biomarkers suitable for FFPE sample sorting should be tested to accurately distinguish tumor cells from nonneoplastic cells.

Supplementary Information

The online version contains supplementary material available at https://doi.org/10.1186/s12575-025-00262-9.

Supplementary Material 1

Acknowledgements
We thank You Li for helping in the analysis of sequencing data.

Author Contributions
The study was designed by Hongyan Liao. FACS and ChIP-seq were performed by Nenggang Jiang and Huan Tao. The manuscript was written by Nenggang Jiang, Zhihao Wen and Hongyan Liao. All authors reviewed the manuscript and approved its submission.

Funding
This study was funded by the Science and Technology Project of Sichuan Province of China (Grant No. 2023NSFSC1484) and the 1•3•5 project for disciplines of excellence-Clinical Research Fund, West China Hospital, Sichuan University (Grant No. 2023HXFH034).

Data Availability
Sequence data that support the findings of this study have been deposited in NCBI with the primary accession code PRJNA1161013. Other data will be made available on request.

Declarations

Ethics Approval and Consent to Participate
The study received approval from the Ethics Committee of West China Hospital of Sichuan University.

Consent for Publication
Not applicable.

Competing Interests
The authors declare no competing interests.

Received: 14 November 2024 / Accepted: 13 January 2025
Published online: 22 January 2025

References

1. Bradner JE, Hnisz D, Young RA. Transcriptional addiction in Cancer. Cell. 2017;168(4):629–43.
2. Shlyueva D, Stampfel G, Stark A. Transcriptional enhancers: from properties to genome-wide predictions. Nat Rev Genet. 2014;15(4):272–86.
3. Whyte W, Orlando DA, Hnisz D, et al. Master transcription factors and mediator establish super-enhancers at key cell identity genes. Cell. 2013;153(2):307–19.
4. Blayney J, Francis H, Rampasekova A, et al. Super-enhancers include classical enhancers and facilitators to fully activate gene expression. Cell. 2023;186(26):5826–39.
5. Lovén J, Hoke HA, Lin CY, et al. Selective inhibition of tumor oncogenes by disruption of super-enhancers. Cell. 2013;153(2):320–34.
6. Teste B, Champ J, Londono-Vallejo A, et al. Chromatin immunoprecipitation in microfluidic droplets: towards fast and cheap analyses. Lab Chip. 2017;17(3):530–7.
7. Robertson G, Hirst M, Bainbridge M, et al. Genome-wide profiles of STAT1 DNA association using chromatin immunoprecipitation and massively parallel sequencing. Nat Methods. 2007;4(8):651–7.
8. Mardis ER. ChIP-seq: welcome to the new frontier. Nat Methods. 2007;4(8):613–4.
9. Do H, Dobrovic A. Sequence artifacts in DNA from formalin-fixed tissues: causes and strategies for minimization. Clin Chem. 2015;61(1):64–71.
10. O'Rourke M, Padula MP. Analysis of formalin-fixed, paraffin-embedded (FFPE) tissue via proteomic techniques and misconceptions of antigen retrieval. Biotechniques. 2016;60(5):229–38.
11. Zhang Y, Zhang Z. The history and advances in cancer immunotherapy: understanding the characteristics of tumor-infiltrating immune cells and their therapeutic implications. Cell Mol Immunol. 2020;17(8):807-21.
12. Romano O, Peano C, Tagliazucchi GM, et al. Transcriptional, epigenetic and retroviral signatures identify regulatory regions involved in hematopoietic lineage commitment. Sci Rep. 2016;20(6):24724.
13. Cejas P, Li L, O'Neill NK, et al. Chromatin immunoprecipitation from fixed clinical tissues reveals tumor-specific enhancer profiles. Nat Med. 2016;22(6):685–91.
14. Amatori S, Ballarini M, Faversani A et al. PAT-ChIP coupled with laser microdissection allows the study of chromatin in selected cell populations from paraffin-embedded patient samples. Epigenetics Chromatin. 2014;(7):18.
15. Fanelli M, Amatori S, Barozzi I, et al. Chromatin immunoprecipitation and high-throughput sequencing from paraffin-embedded pathology tissue. Nat Protoc. 2011;6(12):1905–19.
16. Fanelli M, Amatori S, Barozzi I, et al. Pathology tissue-chromatin immunoprecipitation, coupled with high-throughput sequencing, allows the epigenetic profiling of patient samples. Proc Natl Acad Sci USA. 2010;107(50):21535–40.
17. Flora P, Ezhkova E. Cleavage under targets & release using nuclease (CUT&RUN) of histone modifications in epidermal stem cells of adult murine skin. Methods Mol Biol. 2024;2736:9–21.
18. Lam K, Brick K, Cheng G, et al. Cell-type-specific genomics reveals histone modification dynamics in mammalian meiosis. Nat Commun. 2019;10(1):3821.
19. Jiang N, Chen C, Gong Q, et al. Flow cytometric sorting coupled with exon capture sequencing identifies somatic mutations in archival lymphoma tissues. Lab Invest. 2017;97(11):1364–74.
20. Zhang Y, Liu T, Meyer CA, et al. Model-based analysis of ChIP-Seq (MACS). Genome Biol. 2008;9(9):R137.
21. Shi J, Hou S, Fang Q, et al. PD-1 controls follicular T helper cell positioning and function. Immunity. 2018;49(2):264–e744.
22. Font-Tello A, Kesten N, Xie Y, et al. FiTAc-seq: fixed-tissue ChIP-seq for H3K27ac profiling and super-enhancer analysis of FFPE tissues. Nat Protoc. 2020;15:2503–18.
23. Rudd CE, Schneider H. Unifying concepts in CD28, ICOS and CTLA4 co-receptor signalling. Nat Rev Immunol. 2003;3(7):544-56.
24. Cheng Y, Schorey JS. Extracellular vesicles deliver < i > Mycobacterium RNA to promote host immunity and bacterial killing. EMBO Rep. 2019;20(3):e46613.
25. Chavez J, Foss FM, William BM, et al. Targeting the Inducible T-cell costimulator (ICOS) in patients with Relapsed/Refractory T-follicular helper phenotype peripheral T-cell and angioimmunoblastic T-cell lymphoma. Clin Cancer Res. 2023;29(10):1869–78.
26. Lee G, Jun Y, Jeon YK, et al. Mice transgenic for human CTLA4-CD28 fusion gene show proliferation and transformation of ATLL-like and AITL-like T cells. Oncoimmunology. 2022;11(1):2015170.
27. Whyte WA, Orlando DA, Hnisz D, et al. Master transcription factors and mediator establish super-enhancers at key cell identity genes. Cell. 2013;153(2):307–19.
28. Kaneko S, Mitsuyama T, Shiraishi K, et al. Genome-wide chromatin analysis of FFPE tissues using a Dual-Arm Robot with clinical potential. Cancers (Basel). 2021;13(9):2126.
29. Dou Z, Chau M, Muder D, et al. Optimized protocols for in situ hybridization, immunohistochemistry, and immunofluorescence on skeletal tissue. Acta Histochem. 2021;123(5):151747.
30. Fei M, Ye Q, Yu Y, et al. Cytopathological characteristics of angioimmunoblastic T-cell lymphoma diagnosed by fine needle aspiration. Cytopathology. 2022;33(4):499–504.
31. Chiba S, Sakata-Yanagimoto M. Advances in understanding of angioimmunoblastic T-cell lymphoma. Leukemia. 2020;34(10):2592-606.
32. Zhang S, Postnikov Y, Lobanov A, et al. H3K27ac nucleosomes facilitate HMGN localization at regulatory sites to modulate chromatin binding of transcription factors. Commun Biol. 2022;5(1):159.
33. Melssen MM, Sheybani ND, Leick KM et al. Barriers to immune cell infiltration in tumors. J Immunother Cancer. 2023;11(4).

Publisher's Note